X-RAY DIFFRACTION ANALYSIS OF CYTOCHROME b_5 RECONSTITUTED IN EGG PHOSPHATIDYLCHOLINE VESICLES

L. M. RZEPECKI, P. STRITTMATTER, AND L. G. HERBETTE*
*Department of Biochemistry and *Department of Medicine, University of Connecticut Health Center, Farmington, Connecticut 06032*

ABSTRACT Cytochrome b_5 was reconstituted asymmetrically into large unilamellar egg phosphatidylcholine vesicles. Asymmetry was preserved after sedimentation and partial dehydration to form oriented stacks of membranes. The periodicity of the centrosymmetric unit cell ranged between 145 and 175 Å, depending upon the water content of the oriented multilayer. X-ray diffraction data were collected to a resolution of 12 Å and phase factors were unambiguously assigned by q swelling analysis to a resolution of 15 Å. The lower-resolution profile structures clearly showed a highly asymmetric single membrane containing the heme peptide segment of the cytochrome on one side of the membrane bilayer. The higher-resolution data were also analyzed and profile structures were compared with various models for the distribution of cytochrome b_5 nonpolar peptide within the membrane bilayer region. The data favor an asymmetric distribution of protein mass within the membrane bilayer.

INTRODUCTION

Cytochrome b_5 is an electron carrier participating in a number of oxidation-reduction reactions in the endoplasmic reticulum. Using electrons from cytoplasmically generated reduced pyridine nucleotides, several reductases reduce cytochrome b_5. In turn, cytochrome b_5 diffuses in the plane of the membrane and transfers electrons to other enzyme systems, such as the Δ^9 fatty acyl desaturase (1) and cytochrome P-450 (2), and may also act as a reductant in Δ^6 fatty acid desaturation (3), cholesterol biosynthesis (4), plasmalogen biosynthesis (5), and elongation of fatty acids (6).

The ability of cytochrome b_5 to interact with a number of distinct enzymes is related to its amphipathic nature. The NH_2-terminal catalytically active domain (11,000 mol wt), which binds the heme moiety, is attached by a 9–10 amino acid sequence to a COOH-terminal nonpolar domain (5,000 mol wt) essential for membrane binding. This amino acid linking sequence may confer sufficient flexibility on the cytochrome to permit the diverse interactions required of it.

The heme peptide can be proteolytically separated from the nonpolar peptide and has been extensively characterized by chemical and x-ray crystallographic methods (7, 8). The structure of the nonpolar peptide within the lipid bilayer has not yet been determined directly. Several studies using enzymic and chemical probes (9) suggest that the nonpolar peptide forms a loop within the bilayer, with both the COOH- and NH_2-termini exposed to water on the same side of the membrane. Structural modeling techniques have been used to propose that the bulk of the nonpolar peptide resides at the center of the bilayer with a *cis*[1] configuration (9). In contrast, studies by Takagaki et al. (10, 11) using cross-linking by photoactivatable lipid probes suggested that the nonpolar peptide spans the membrane. In low-resolution neutron diffraction and solution scattering studies, Gogol et al. (12) and Gogol and Engelman (13) analyzed both a cytochrome b_5 membrane system with an average multilayer unit cell repeat of 200 Å, and vesicles containing cytochrome b_5. They were unable to distinguish reliably between the *cis*-model,[1] where the bulk of the protein resides at the center of the bilayer, and a *trans* model,[1] which assumed a uniform distribution of protein mass across the bilayer.

The x-ray diffraction studies presented in this paper were undertaken to characterize the reconstituted cytochrome b_5 membrane, where the cytochrome is unidirectionally oriented within the membrane bilayer. Such studies require the preparation of highly ordered multilayers composed of centrosymmetric unit cells where the unit cell

Address correspondence to Dr. L. M. Rzepecki, Department of Biochemistry, University of Connecticut Health Center, Farmington, CT 06032.

[1] *Cis* defines a protein configuration where the NH_2- and COOH-termini are on the same side of the membrane bilayer. *Trans* defines a protein configuration where the NH_2- and COOH-termini are on opposite sides of the membrane bilayer. Neither of these configurations defines the protein mass distribution across the membrane bilayer. However, by definition, the *trans* configuration requires that protein mass be distributed across the entire width of the membrane; this could be a uniform or asymmetric distribution. The *cis* configuration neither requires nor excludes a protein mass distribution across the entire width of the membrane; this distribution can be uniform or asymmetric.

comprises two apposed asymmetric membranes. In a highly asymmetric membrane with >95% unidirectional orientation of the cytochrome, the distribution of the nonpolar peptide can be modeled at relatively high resolution. The reconstitution methods employed here, involving the insertion of cytochrome b_5 into large unilamellar vesicles, allowed the formation of functionally asymmetric samples, and the methods employed in handling the samples after the formation of oriented multilayers preserved the initial structural asymmetry. A detailed analysis of these membranes could answer some of the remaining structural questions about cytochrome b_5 and thus help clarify the nature of the interactions between the cytochrome and other protein components of the electron transfer chain.

MATERIALS AND METHODS

Preparation of Cytochrome b_5: Egg Phosphatidylcholine Vesicles

Cytochrome b_5 was purified from Black Angus steer liver as described (14). Cytochrome b_5 reductase was purified from the same source as described previously (15), with the addition of an ADP-agarose (P.L. Biochemicals Inc., Piscataway, NJ) affinity chromatography step (16). Phosphatidylcholine was extracted from egg yolks by the method of Bangham et al. (17), purified on an alumina column (18), and stored at −20°C in chloroform in the presence of 0.1% butylated hydroxytoluene (Sigma Chemical Co., St. Louis, MO). Phospholipid was determined by the method of Chen et al. (19).

Small unilamellar egg phosphatidylcholine vesicles were prepared by sonication in a bath sonicator (Bransonic 12, Branson Sonic Power Co., Danbury, CT). Buffers containing 0.1 M NaCl, 0.1 mM EDTA, and 20 mM Tris acetate, pH 8.1, were used throughout. The vesicle suspension was sedimented at 100,000 *g* for 3 h to remove residual multilamellar liposomes, which would interfere with the diffraction analysis. The upper half of the supernatant was removed with a Pasteur pipette and used in the preparation of samples for x-ray diffraction. Small vesicles were converted to large unilamellar vesicles (LUVs) by the addition of 10% wt/vol sodium deoxycholate (Aldrich Chemical Co., Milwaukee, WI) to a lipid/deoxycholate ratio of 2:1 (20). The resulting suspension was incubated at 30°C for 15 min to allow LUVs to form. Vesicles were then diluted to a concentration of 2 mM phospholipid and concentrated cytochrome b_5 was added to give a lipid/cytochrome b_5 ratio of 10:1. These suspensions of LUVs and cytochrome b_5 were incubated for periods of 12–24 h at 30°C. Vesicles containing reconstituted cytochrome b_5 were separated from unbound cytochrome b_5 and from deoxycholate on 50 vol of Sepharose 4B (P.L. Biochemicals Inc.) pre-equilibrated in the same buffer as previously described (20). Cytochrome b_5 was estimated by measuring the absorbance difference between reduced and oxidized cytochrome at 424 nm (ϵ_{mM} = 100). Deoxycholate was estimated by incorporating ^{14}C-labeled deoxycholate (Mallinckrodt Nuclear, St. Louis, MO) into the vesicles during the formation of LUVs. The orientation of reconstituted cytochrome b_5 was determined by measuring the amount of cytochrome b_5, which could be reduced upon addition of NADH and cytochrome b_5 reductase, to which the membrane is impermeable, relative to the total amount of cytochrome b_5 reduced by the addition of a few crystals of sodium dithionite, which can penetrate the membrane.

Electron Microscopy

Membrane Vesicles. Vesicles were centrifuged at g_{av} = 100,000 for 1 h in an SW27 swinging bucket rotor and the pellet was immediately fixed in a solution of 2% OsO_4 in 0.1 M cacodylate buffer, pH 7.0, then washed briefly with water and incubated with 1% aqueous uranyl acetate at 60°C for 30 min. After dehydration with ethanol, the pellet was embedded in Polybed 812. Thin sections were cut with a diamond knife on an MT2-B ultramicrotome, mounted on copper grids and counter-stained with uranyl acetate and lead citrate. The sections were examined with an electron microscope (Hu 11-E; Hitachi, Ltd., Tokyo, Japan) at an accelerating voltage of 75 kV.

Thin-Section Membrane Multilayers. Hydrated, oriented multilayers were prepared as described below. After these membrane multilayers were partially dehydrated at controlled humidities at 5°C for ~20 h, a vial of 2% osmium was placed in the relative humidity chamber and the membrane multilayer was allowed to fix via the vapor phase for 2–4 h (21). These fixed multilayers were then simultaneously counter-stained with 1% uranyl acetate and dehydrated, and then embedded as described previously (22). Thin sections were cut approximately parallel to the sedimentation axis of the multilayer.

Preparation of Samples for Diffraction

Suspensions of large unilamellar vesicles (~400 nmol phospholipid) containing reconstituted cytochrome b_5 were sedimented at 100,000 *g* onto aluminum foil in Lucite sedimentation cells as previously described (22). The aluminum foils were then affixed to curved glass sample-holders (23) and sealed in vials over saturated salt solutions to provide a relative humidity in the range 80–96% at 8°C. After dehydration for periods of 12–48 h, the sample-holders were mounted for diffraction in sealed brass canisters (24, 25) with aluminum windows to permit passage of the x-ray beam. The temperature during x-ray exposures was controlled (±0.2°C) over a range of 10–15°C. Relative humidity was maintained with the appropriate salt solutions present in the sealed canisters.

Lamellar X-Ray Diffraction Data Collection, Reduction, and Analysis

Oriented membrane multilayers of reconstituted cytochrome b_5 were exposed to a collimated, monochromatic x-ray beam (Cuk_α x-rays, λ = 1.54 Å, $K_\alpha 1$ and $K_\alpha 2$ being unresolved) from a Rigaku-Denki RU3 rotating anode generator (Rigaku/USA, Inc., Danvers, MA) using one vertical Franks' mirror on a custom-built diffraction camera. The curved multilayer specimen (temperature and relative humidity regulated) was oriented with respect to the x-ray beam at near-grazing incidence in order to obtain the lamellar meridional diffraction pattern, which was recorded on x-ray–sensitive film (Kodak no-screen type NS5T).

All lamellar diffraction patterns recorded on film and used for analysis were quantitated on a one-dimensional scanning densitometer (Helena Laboratories, Beaumont, TX). A two-dimensional laser scanning densitometer (Biomed Instruments, Inc., Fullerton, CA) was used only qualitatively to investigate the degree of mosaic spread of the lamellar reflections. Diffraction patterns were integrated on the one-dimensional scanner, using a slit height much lower than the height of the lamellar reflection, by scanning through the center of each reflection arc along the lamellar meridional axis. On the two-dimensional scanner, the entire reflection arc on the lamellar meridional axis of the film was scanned using a point source beam with a resolution of 10 μm and the digitized data set was then graphically displayed. The digitized intensity data [$I(s)$] from the one-dimensional densitometer were transferred directly to computer memory. The resulting one-dimensional intensity functions were background corrected by fitting a background curve generated by a spline-fit algorithm (26). This calculated background curve was subtracted digitally from the total intensity function providing a background-corrected intensity function, $I_c(s)$. The resulting lamellar intensities were integrated using a Gaussian fitting routine and corrected by $s^2 = (2\sin\theta/\lambda)^2$. The origin of these correction factors for x-ray diffraction data has been discussed previously (21). The Gaussian fitting procedure was essential since, because of a small degree of lattice disorder (27), the full

width at half-maximum of the lamellar intensities increased by 50% from $I(h = 1)$ to $I(h = 12)$. These properly determined integrated intensities were then used in the following analysis. Unit cell dimensions (d) were obtained from the spacing of these lamellar reflections or by calculation of the appropriate autocorrelation functions. The integrated lamellar intensities [$I(h = 1–10)$], where h is the diffraction order index, were phased by the swelling method (28), using a previously described algorithm (29). The phasing procedure was carried out in two steps. The most probable phase combination for intensities [$I(h = 1–6)$] was obtained by evaluating all possible phase combinations using this algorithm (29). Fixing the phases for these intensities, all possible phase combinations for [$I(h = 7–10)$] were then evaluated. The most probable phase combination for [$I(h = 1–10)$] was thus obtained. The phase factor for $I(h = 12)$ was not assigned unambiguously (see Results). The corrected structure factors, $F(h)$, were used in a Fourier series according to Guinier (30) to provide the corresponding electron density profile structures at ~15 Å resolution.

Modeling of Electron Density Profiles

Step-function equivalent profiles were fitted to the experimental profile structures by the following procedure. The calculated step-function equivalents were Fourier-transformed once to generate the continuous structure factor function, which was truncated at a resolution equivalent to that of the experimental data (using 10 diffraction orders). This truncated transform was then Fourier-transformed a second time to generate a calculated continuous profile structure. The calculated profile structures were compared with the experimental profiles by a least-squares fit (R value), and the calculation was terminated when the fit was less than or equal to the experimental noise of the lamellar intensity data (24).

Theoretical electron density profiles for various models of reconstituted cytochrome b_5 within the membrane bilayer region were calculated by the following procedure. The unit volume for the membrane was defined as that which contains nonpolar peptide with the appropriate complement of lipid derived from the chemically determined lipid/protein ratio. Protein volume was calculated for each bilayer segment from the amino acid volumes given by Cohn and Edsall (31) according to the known amino acid sequence (32). The contribution of protein to the electron density was calculated by a summation of the electron densities of the amino acids (33) present in each bilayer segment. The electron densities were derived from the amino acid volumes and ranged between 0.37 and 0.52 e/Å^3. Lipid volume was taken to be 1,253 Å^3/lipid (34), and was divided into hydrophobic and hydrophilic regions in the ratio 2:1. Lipid electron densities were taken to be in the range 0.39–0.45 e/Å^3 for the headgroup, 0.296 e/Å^3 for the fatty acyl chains, and 0.232 e/Å^3 for the terminal methyl region (35). The distribution of protein across the bilayer was arbitrarily fixed for various models, while the lipid distribution was varied such that the volumes of the inner and outer leaflets remained equal (i.e., the average cross-sectional area for the membrane unit volume was constant). Theoretical electron density profiles for various protein models thus generated were compared with the step-function equivalent profiles derived from the experimental profile structures.

Materials

All chemicals used were reagent grade. Deionized water was glass-distilled before use.

RESULTS

Reconstitution of cytochrome b_5 into Egg Phosphatidylcholine Vesicles

Previous attempts to incorporate cytochrome b_5 asymmetrically into large egg phosphatidylcholine vesicles in the presence or absence of deoxycholate had not led to consistent results either because the degree of asymmetry could not be controlled (36) or because cytochrome b_5 could not bind to the vesicles in the "tight binding" configuration thought to mimic in vivo membrane binding (36). Moreover, these initial preparations gave x-ray diffraction patterns with major contributions from phase-separated lipid and lipid/protein aggregates.

In order to overcome these problems, we tried a variety of reconstitution conditions, the most successful of which is presented in detail in Materials and Methods. Deoxycholate was required to bind cytochrome b_5 tightly to vesicles. The asymmetry of cytochrome b_5 in the bilayer was controlled by reducing the absolute concentration of lipid and deoxycholate during reconstitution to a level equal to or smaller than the critical micellar concentration of deoxycholate. The homogeneity of samples, as indicated by single-repeat diffraction patterns, was greatly improved by taking precautions to ensure that the small unilamellar vesicles at the start of the reconstitution procedures were free from contamination by multilamellar liposomes. The relative concentrations of lipid and cytochrome b_5 during reconstitution were chosen to ensure maximal binding of the cytochrome to lipid bilayers.

The elution profile of reconstituted cytochrome b_5 vesicles from a Sepharose 4B column is shown in Fig. 1. The reconstitution procedure resulted in a suspension of large, unilamellar vesicles free from deoxycholate and unbound cytochrome b_5. Electron microscopy of vesicle dispersions showed that the vesicle population was fairly uniform in size (800–1,000 Å diam, data not shown). The lipid/cytochrome b_5 molar ratios in samples used for diffraction ranged between 22 and 25, which appeared to be a saturating concentration of cytochrome b_5 in the membrane. Longer incubations (60 h) to bind cytochrome b_5 to vesicles did not increase the amount of cytochrome bound. The incorporation of cytochrome b_5 into unilamellar membrane vesicles was highly asymmetric (>98%). The bound

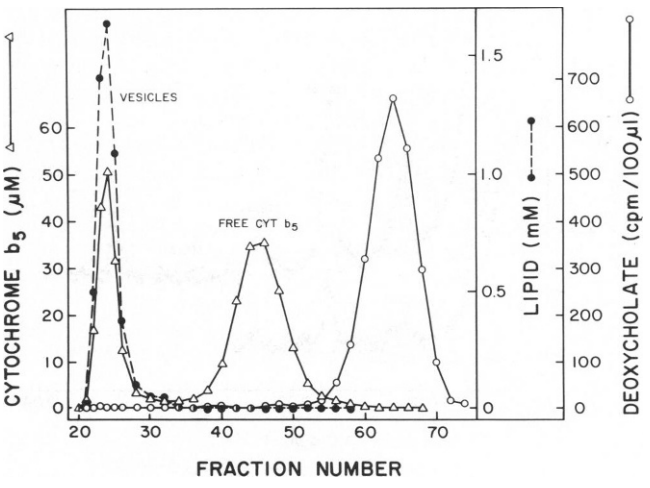

FIGURE 1 Elution profile of cytochrome b_5 vesicles from Sepharose 4B. Cytochrome b_5 (△), phospholipid (●), ^{14}C-labeled deoxycholate (○).

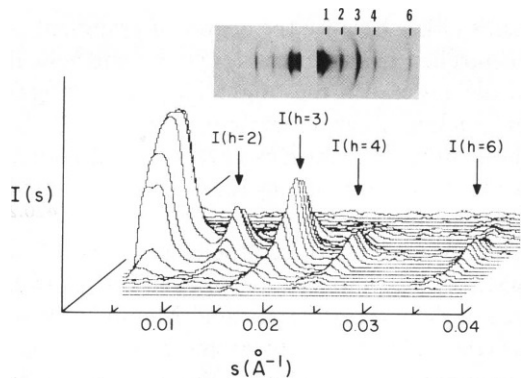

FIGURE 2 Pseudo–three-dimensional representation of the low-angle diffraction pattern from cytochrome b_5 membrane multilayers using a two-dimensional scanning densitometer showing diffraction orders $I(h = 1–6)$; $I(h = 1)$ for this scan was saturated on the film. *Inset*: low-angle x-ray diffraction pattern from which the scan was taken; d = 156 Å.

cytochrome could not be transferred to other vesicles (36), nor could it be released from vesicles by carboxypeptidase Y (36, 37), which will release loosely but not tightly bound cytochrome b_5; this demonstrates that it was tightly bound to the membrane (data not shown).

X-Ray Diffraction Analysis

Membrane multilayers composed of flattened cytochrome b_5 vesicles dehydrated at 96% relative humidity gave clearly defined, reproducible diffraction orders that indexed on a single unit cell repeat within the range of 145–175 Å, depending on the water content of the multilayer sample. For some samples, lamellar meridional diffraction was observed to a resolution of ~15 Å (10 diffraction orders). At lower water content, the resolution was extended to ~12 Å (12 diffraction orders). In Fig. 2, a pseudo–three-dimensional plot of a diffraction pattern was recorded on a two-dimensional scanning densitometer clearly showing the mosiac spread and well-defined shape of the lamellar meridional reflections. The same diffraction pattern was also scanned on the one-dimensional densitometer providing the total lamellar intensity function $[I(h = 1–6)]$ (a typical example of which is shown in Fig. 3 *A*), which was then background corrected (Fig. 3 *B*). Higher-angle data were often observed and a typical example of the background-corrected intensity function is shown in Fig. 4. At higher angles, in the vicinity of $I(h = 8–12)$, a slowly varying background was sometimes observed underlying the lamellar reflections. This background was subtracted out by a spline-fitted curve as described in Materials and Methods. The origin of this slowly oscillating background is not known, but a portion of it is apparently camera background as demonstrated by control exposures with no sample. The remaining background could arise either from some form of disorder (other than lattice disorder) or from equatorial scattering that arced to the lamellar meridional axis. However, as can be seen, these diffraction patterns consisted of relatively sharp odd- and even-order reflections with very strong odd-order reflections resting on this background.

Electron micrographs of equivalent samples showed extensive arrays of multilamellar stacks with an asymmetric staining pattern of an ~130 Å repeat, which must correspond to the dehydrated state of a unit cell composed of two asymmetric membranes (Fig. 5). The considerably lower periodicity observed in thin-sectioned multilayers probably reflects a much higher degree of dehydration during the fixation process. This confirmed the centrosymmetry of the multilayer unit cell observed in x-ray diffraction experiments for repeats within the range of 145–175 Å. Thus, for x-ray diffraction, the unit cell must contain the closely apposed membranes of a flattened vesicle with internal and external water layers. Other samples processed for electron microscopy, however, showed the presence of multiple unit cell repeats within the multilayer

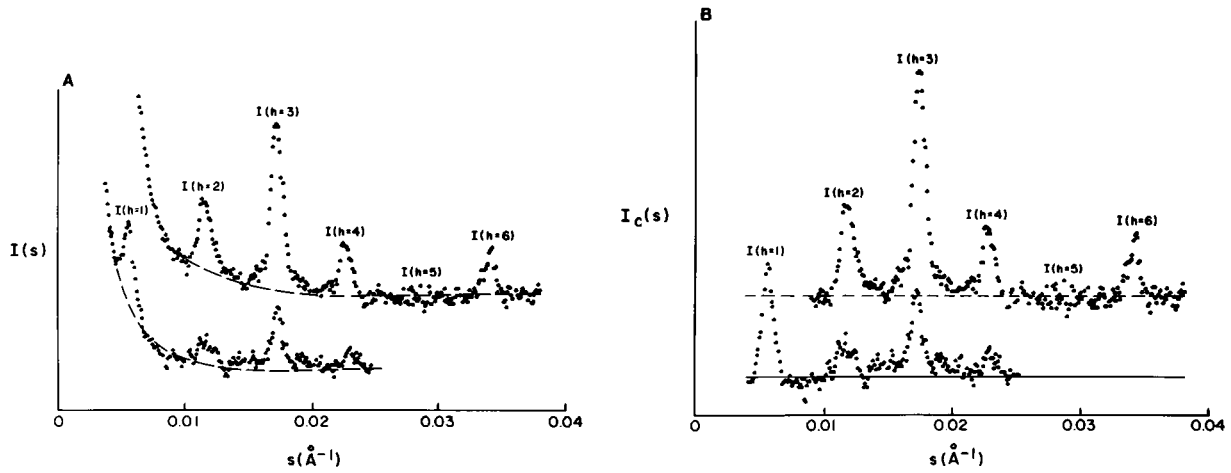

FIGURE 3 One-dimensional densitometer scan of a low-angle diffraction pattern from cytochrome b_5 membrane multilayers at 93% relative humidity. d = 164 Å. (*A*) Densitometer scan of the first and second films from a single exposure. The dashed line is the spline-fitted background curve. (*B*) Background-corrected low-angle intensity function.

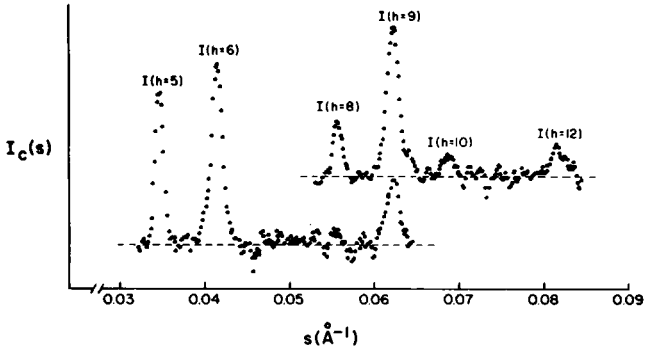

FIGURE 4 Background-corrected higher-angle intensity function obtained from a diffraction pattern from cytochrome b_5 membrane multilayers at relative humidity of 88%; d = 145 Å.

TABLE I
SWELLING EXPERIMENT INTENSITY VALUES $I(h)$

h	D = 163.3	154.2	144.8
1	967.2	232.1	460
2	253.3	65.5	309.1
3	416	95.1	420.2
4	107	20.4	56.4
5	7.1	4.65	25
6	78.9	16.4	33.9
7	12	0	0
8	0	0	4.2
9	20.3	8.92	14.1
10	13.9	3.71	2.16
11	0	0	0
12	0	0	3.12

sample, including a repeat that must correspond to a symmetric membrane (100 and 200 Å unit cell repeats; see the Appendix, Fig. 9). These latter unit cell repeats were observed in x-ray diffraction patterns derived from samples that had deteriorated, but the periodicities and relative intensities of the diffracted orders were quite distinct from those patterns corresponding to the 145–175 Å unit cell repeat range. Thus, the presence of the various unit cell repeats corresponding to unit cells with different compositions (see Appendix) could be easily distinguished in x-ray diffraction patterns, and only diffraction patterns with a single unit cell repeat in the range of 145–175 Å were analyzed in detail.

A swelling analysis was carried out in order to phase the lamellar reflections. Three sets of intensity data of 96, 93, and 88% relative humidity were used in the analysis (Table I). These relative humidities corresponded to unit cell repeats of 163, 154, and 145 Å. In order to facilitate the phasing analysis, only the first six orders [$I(h$ = 1–6)] were included in the initial swelling analysis. This swelling analysis was performed on all possible pairs of unit cell repeats obtained at the three relative humidities in order to assign unambiguous phase factors to the experimentally obtained structure factors. The algorithm devised by Stamatoff and Krimm (29) was used to compute the Δ value for all possible phase combinations, and the five most probable phase combinations were ranked by their appropriate values. This algorithm provides a hierarchy of the more probable phase combinations and hence the unit cell profile structures, with the most probable profile structure possessing the least deviation (smallest Δ) with variations

FIGURE 5 Electron micrograph of cytochrome b_5 membrane multilayers sedimented and dehydrated by methods identical to those used for x-ray diffraction studied; an asymmetric banding pattern (two membranes per repeat unit) of 130 Å was measured. The arrows mark the external surfaces of one collapsed vesicle. The origin of external and internal surfaces could be determined by identifying ends of collapsed vesicles where the membrane is seen to loop around. The horizontal bar represents 600 Å.

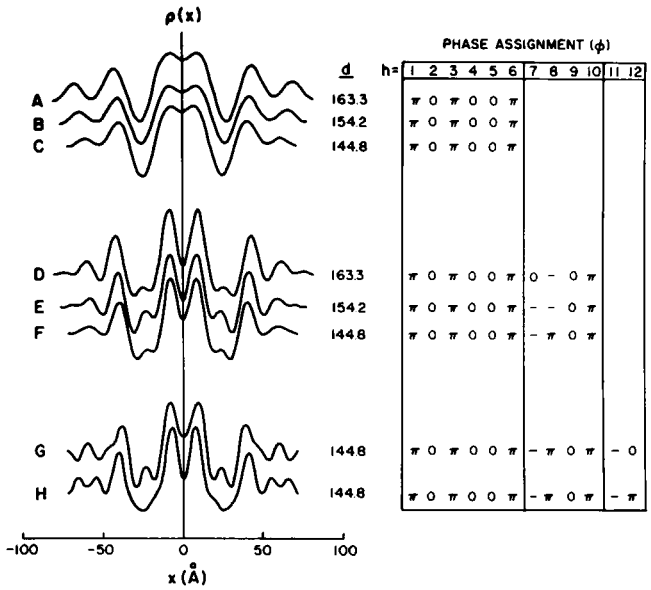

FIGURE 6 (A–C) Low-resolution (26 Å) electron density profiles for the reconstituted cytochrome b_5 membrane as a function of hydration. The profiles were calculated using the corrected intensities $I(h$ = 1–6) with the phase combination of π, 0, π, 0, 0, π, determined by swelling with d = 164 (A), 154 (B), and 145 (C) Å. (D–F) Higher-resolution (15 Å) electron density profiles for the reconstituted cytochrome b_5 membrane as a function of hydration (same d values as in A–C). Profiles were calculated using intensities $I(h$ = 1–10) with phases assigned by the swelling method. (G and H) Electron density profiles calculated using the phase assignment of 0 (G) or π (H) for $I(h$ = 12).

in multilayer unit cell repeats. The phase combination, π, 0, π, 0, 0, π was obtained for $I(h = 1–6)$ for all three unit cell periodities. The electron density profile, derived from this low-resolution (26 Å) analysis, is shown on a relative electron density scale in Fig. 6 (*A–C*), and was found to be consistent with a unit cell containing two asymmetric membranes corresponding to the two apposed membranes of the flattened vesicle.

After fixing the phases of the first six orders to give a low-resolution electron density profile, the swelling analysis was extended to the higher orders [$I(h = 7–10)$]. The most probable phase combination for $I(h = 7–10)$ was dependent on the unit cell repeat since not all orders were observed for each repeat period. The resulting higher-resolution profile structures are shown in Fig. 6, *D–F*. These profiles are similar in nature to the lower-resolution profile structures shown in Fig. 6, *A–C*. They also indicate that ~90% of the swelling had occurred primarily at $x = \pm D/2$, since, for a total unit cell repeat change of 18 Å (Fig. 6, *D* vs. *F*), the spacing between the inner electron-dense maxima near $x = 0$ Å was changed by ~2 Å. An additional high-angle reflection [$I(h = 12)$] was observed at the lowest humidity, 88% (Fig. 4 and Table I). Although this reflection was excluded from the phasing analysis, the two possible electron density profiles at 12 Å resolution were generated using the two alternative phase assignments of $I(h = 12)$ of 0 or π (Fig. 6, *G* and *H*). Either phase assignment yields profiles consistent with the low-resolution (26 Å) electron density profile. However, the profile given in Fig. 6 *G* with $\phi = 0$ most resembles the profile structures given in Fig. 6, *D–F*.

DISCUSSION

Experimental Profile Structure

Cytochrome b_5 was reconstituted asymmetrically, in the presence of deoxycholate, into large, unilamellar egg phosphatidylcholine vesicles. After deoxycholate removal, careful sedimentation and partial dehydration of these vesicles formed oriented multilayers that were shown to be composed of centrosymmetric double-membrane repeat units. The periodicities of such samples varied between 145 and 175 Å, depending upon the water content of the oriented multilayer. A swelling analysis over this range of unit cell repeats allowed the direct phasing of the first six orders to give lower-resolution (26 Å) (Fig. 6, *A–C*) and, subsequently, higher-resolution (15 Å) (Fig. 6, *D–F*) electron density profiles. This analysis revealed two closely apposed lipid bilayers in the unit cell, with electron density maxima at the external edges of the unit cell, which is consistent with electron microscopy images of thin-sectioned, fixed multilayers. These maxima, near the edge of the unit cell (near $\pm D/2$), probably represent the heme peptide of cytochrome b_5. This highly asymmetric membrane structure demonstrates that the cytochrome must retain the original asymmetric orientation in the lipid bilayer, which characterizes vesicles before the formation of the oriented multilayers. This profile is qualitatively similar to one derived by Blaurock (38) for a membrane system incorporating cytochrome *c* and a mixture of phospholipids, and by Pachence et al. (39) in a system incorporating cytochrome *c* and photoreaction centers, and is thus consistent with the observation that the heme peptide is excluded from the bilayer and contained in the aqueous phase. The higher-resolution (15 Å) electron density profiles (Fig. 6, *D–F*) obtained showed some fine structure in the heme peptide region of the unit cell (within $D/3 \leq x \leq D/2$). Since the heme peptide can be modeled as a cylinder with the heme moiety, which contains the electron-dense ferric atom, at one end (7), this fine structure may correspond to one or more orientations of the heme peptide with respect to the membrane plane.

The two electron-dense maxima within $0 \leq x \leq D/3$ of the electron density profile at 15 Å resolution, probably correspond to the phospholipid headgroups of the membrane bilayer, and their separation was 33 Å. The asymmetry in the electron density profile within this region (hydrocarbon core) also suggests that there is a distinct asymmetry in the distribution of protein and hence a corresponding asymmetry in the distribution of phospholipid within the membrane bilayer (24). Although the phase of $I(h = 12)$ is ambiguous, it is apparent that a phase assignment of $\phi = 0$ yielded an electron density profile (Fig. 6 *G*), at 12 Å resolution, with structural features most consistent with the profile structures obtained at 15 Å resolution (Fig. 6, *D–F*). Additional fine structure is apparent in the region $D/3 \leq x \leq D/2$, but it is uncertain whether this fine structure is real or is due to truncation artifacts.

Model Calculations

Various models for the structure of the nonpolar peptide in the bilayer have been proposed (8, 11, 12). To test these models, step-function equivalent profiles were fitted to the experimentally determined electron density profiles and compared with the theoretical electron density profiles predicted by the models (see Materials and Methods). The step-function equivalent profile fitted, with an R value < 1%, to the electron density profile at 15 Å resolution (Fig. 6 *D*, $0 \leq x \leq D/2$) is shown in Fig. 7 *A*. This step function depicts a bilayer with a minimum thickness of 38 Å, a highly asymmetric hydrocarbon core with a low-density trough in the outer monolayer, and fine structure corresponding to the heme peptide region for $D/3 \leq x \leq D/2$ of the unit cell.

Of all the conceivable models for the structure of the nonpolar peptide, two basic types, shown schematically in Fig. 7 *D*, were selected as being the most likely candidates, and were examined in some detail. Type I models were calculated assuming a relatively uniform distribution of protein mass across the bilayer. Such models included those with a single *trans*-membrane α-helix inserted to different depths in the membrane bilayer, with the NH_2

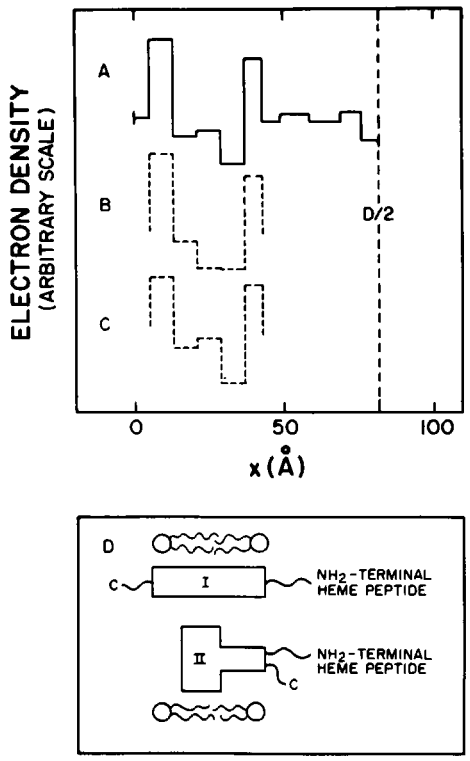

FIGURE 7 Models for the experimental electron density profiles at a resolution of 15 Å. (*A*) Fitted step function to the electron density profile of Fig. 6 *D* ($0 \leq x \leq D/2$). *R* value = 0.6%. (*B*) Calculated model step function of a bilayer with a uniform protein cylinder representing a single *trans*-membrane α-helix, and with a lower lipid density (less lipid) in the outer compared with the inner monolayer. (*C*) Calculated model step function of a bilayer containing a bulk protein mass extending from the bilayer center into the inner monolayer, with the NH_2- and COOH-termini both at the outer surface of the membrane bilayer. (*D*) Different models proposed for the nonpolar peptide: I, transmembrane α-helix; II, loop model with the NH_2- and COOH-termini on the same side of the membrane bilayer (see Discussion).

and COOH-termini on opposite sides of the bilayer (11). Type II models were calculated assuming that the bulk of the protein mass was located at or near the center of the bilayer and extended to varying depths into the inner monolayer. Such models included those with a *cis*-membrane configuration, with the NH_2- and COOH-termini on the same side of the bilayer as proposed by structural modeling techniques (8), as well as models with a *trans*-membrane orientation. Although the present data do not permit a definitive description of the relative contributions of protein and lipid to the electron density profile, the models predict certain features of membrane structure that might be reflected in the experimental electron density profiles.

In the case of type I models, the shape of the model electron density step function was dominated by the lipid component, since the protein mass was uniformly distributed across the bilayer, resulting in profile structures with a relatively symmetrical appearance (not shown). A source of asymmetry could be introduced by arbitrarily varying the lipid content, volume, and electron density of the outer monolayer by 10–20%, but the resulting profiles (see example profile of Fig. 7 *B*) still did not resemble the calculated step-function equivalent profile fitted to the experimental profile structure (Fig. 7 *A*). However, there is no compelling a priori reason to propose such a lipid asymmetry in this case.

In the case of type II models, the protein contribution to the model electron density step function was much more pronounced (not shown). The lipid content and electron density of the outer monolayer were then varied to produce model step functions that resembled the fitted step-function equivalent profile (see example profile of Fig. 7 *C*). It seems reasonable that an asymmetric protein distribution across the bilayer should induce corresponding lipid asymmetry, which would then have to be modeled to achieve a structurally and physically reasonable profile (24).

Clearly, a number of different specific models of either type I or II could generate model profiles similar to those of Fig. 7, *B* and *C*. The models considered in detail, however, serve to illustrate some of the anticipated characteristics of a phospholipid bilayer containing an integrally inserted protein. The "correct" model cannot be selected without knowing the boundary conditions for such parameters as the asymmetry in the numbers of phospholipid molecules in each monolayer of the membrane bilayer, the precise water distribution, and the conformational perturbation of the lipid bilayer by the protein. In addition, although the type I and type II models have been schematically drawn in Fig. 7 *D* as *trans* and *cis* membrane, respectively, in accordance with previously proposed structures, the present data cannot resolve the topology of the nonpolar peptide in the bilayer.

However, on the assumption that the conservative assignment of $\phi = 0$ for I ($h = 12$) (Fig. 6 *G*) is correct, a general consideration of the data seems to exclude a uniform α-helix (or helices) extending across the bilayer. Rather, the data favor an asymmetric distribution of protein mass, with a corresponding lipid asymmetry.

Interpretations of Diffraction Analysis

Some features of the data presented above are strikingly different from those derived from previous neutron diffraction studies (12). Notably, our cytochrome b_5 preparations gave characteristic diffraction periodicities of 145–175 Å, which is considerably lower than the 200 Å periodicity observed by neutron diffraction (12), even though our smallest unit cell repeats were obtained at higher humidities. The reconstituted cytochrome b_5 sample studied by Gogol et al. (12) contained lipid bilayers that were equidistantly spaced within the unit cell (100 Å apart), a finding difficult to reconcile with a membrane system containing an asymmetrically inserted cytochrome b_5 and partially dehydrated to form an oriented multilayer at 75% relative humidity. In contrast, our data show that the inner faces of

the lipid bilayers are closely apposed, as would be expected, with the heme peptide positioned at the outer edges of the centrosymmetric unit cell, which corresponds to the two apposed asymmetric membranes of a flattened vesicle. In addition to these considerations, we show (see Appendix) that it is possible to obtain single-phase diffraction patterns from samples with periodicities of ~100 or 200 Å. Similar periodicities were also found in membrane samples that had originally given the 145–175 Å diffraction pattern, but which had subsequently deteriorated into multi-repeat systems. Electron microscopy of cytochrome b_5 membranes often showed a multiplicity of repeats, with both symmetric and asymmetric membranes present (see Appendix). The difficulties we experienced in obtaining good electron micrographs of cytochrome b_5 membrane samples with a single unit cell repeat further testify to the high lability of this membrane system and its susceptibility to environmental changes, e.g., low humidity (<88%). We have found that the proper handling of samples for diffraction studies required sealed conditions at high humidity, and that sudden or too abrupt humidity variations yielded multi-repeat or 100 or 200 Å repeat samples. Although we have not phased the lamellar intensities for diffraction patterns obtained from samples with periodicities of 100 or 200 Å, generation of all possible profiles that resembled a membrane structure indicated a single symmetric membrane of ~100 Å extent.

We suggest, therefore, that the 100 Å periodicity corresponds to a symmetric membrane, formed at some stage during the partial dehydration of the multilayers, while the 200 Å periodicity corresponds either to two membranes that retain some residual asymmetry or to a condition where the membrane is slightly asymmetrically positioned within the water layers of the half-unit cell. For both unit cell repeats, the protein must be present on both sides of the membrane bilayer (i.e., a bidirectional orientation of the cytochrome). It is likely, then, that the neutron diffraction studies carried out by Gogol et al. (12) used a membrane sample with a considerable degree of symmetry, which would obscure any detail of the structure of the cytochrome b_5 nonpolar peptide within the bilayer.

The *cis*-membrane model for cytochrome b_5 nonpolar peptide previously proposed by Strittmatter and Dailey (8) relied on data that placed the single fluorescent tryptophan 109 residue 20–22 Å from the surface of the bilayer (40), placed the COOH-terminal tyrosine 126 and tyrosine 129 residues at the outer surface of the membrane (9), and predicted the secondary structure from the amino acid sequence (32, 41). Although Takagaki and co-workers (10, 11), using phospholipid cross-linking to the nonpolar peptide, disagreed with this conclusion, their data suffered from low yields of cross-linked protein and a relatively high degree of protein symmetry across the bilayer.

The x-ray diffraction data presented above suggest an asymmetric distribution of protein across the membrane, which is consistent with a *cis*-configuration model for the nonpolar peptide. Although we cannot exclude a *trans*-configuration model, we have established a reconstituted membrane system with the potential to resolve the ambiguities. We have obtained a series of predictive models that can be tested by further x-ray and neutron diffraction measurements. Iodination of tyrosines 126 and 129 at the COOH-terminus of cytochrome b_5 should permit the direct determination of the position of the COOH-terminus in the bilayer. Neutron diffraction studies of membranes reconstituted with either deuterated cytochrome b_5 or deuterated phosphatidylcholine should distinguish the relative mass distributions of protein and lipid across the bilayer. Such information will further restrict the choices of nonpolar peptide models derived from the x-ray diffraction data.

APPENDIX

Our initial x-ray diffraction studies of reconstituted cytochrome b_5–egg phosphatidylcholine membranes demonstrated the difficulty of preparing homogeneous, single-phase membrane samples. These preliminary studies showed that multilayers could be prepared to contain unit cell periodicities in the range of 145–175, 100, and 200 Å, as well as a repeat distance arising from a separated lipid phase (~60 Å). Moreover, samples that had originally given a single unit cell repeat within the range of 145–175 Å often degenerated to multi-repeat systems that included the 100 and 200 Å unit cell repeats. Some samples, however, were characterized from the onset by a single unit cell repeat of either 100 or 200 Å (Fig. 8), and were of some interest as they appeared to correspond to the membrane preparations presented by Gogol et al. (12).

It was not possible to phase the lamellar reflections from samples with homogeneous periodicities of 100 or 200 Å unambiguously by a swelling method since these samples were not stable. However, we generated all the possible electron density profile structures at low resolution using five to six diffraction orders. All these profile structures, which resembled a membrane bilayer structure, indicated a symmetric membrane.

Electron micrographs of many cytochrome b_5 membrane samples showed a multiplicity of unit cell repeats that included asymmetric membranes, symmetric membranes, and separated lipid. An example of a thin-section multilayer containing a symmetric pattern of 70 Å repeat is shown in Fig. 9. This repeat, obtained where the membrane is maximally dehydrated, probably corresponds to the 100 Å repeat seen by x-ray diffraction. Pure lipid bilayers fixed and thin-sectioned under similar conditions yield smaller unit cell repeats (<50 Å). Although the relative predominance of the asymmetric and symmetric membranes varied from sample to sample, most samples processed for microscopy contained both

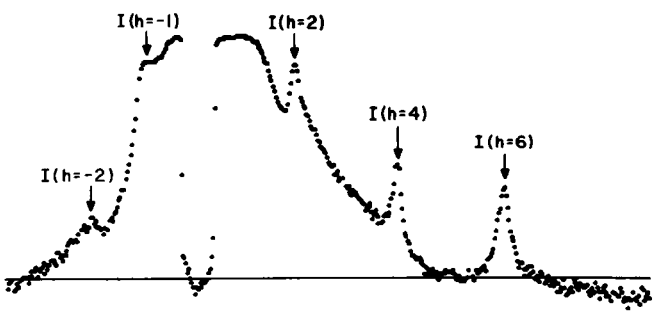

FIGURE 8 One-dimensional densitometer scan of the low-angle x-ray diffraction pattern from reconstituted cytochrome b_5 membrane multilayers at 93% relative humidity; d = 196 Å; note $I(h = -1)$, which indicates that the average unit cell repeat is 196 Å.

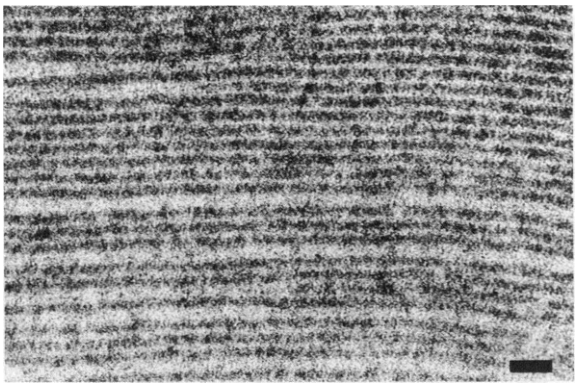

FIGURE 9 Electron micrograph of cytochrome b_5 membrane multilayers sedimented and partially dehydrated similarly to those used for x-ray diffraction, and then fixed for microscopy; a symmetric banding pattern with a repeat of 70 Å was measured. The horizontal bar represents 200 Å.

and this may be due to the rather harsh fixation conditions required to enhance the electron contrast of the cytochrome b_5 samples.

It is probable that the membrane samples characterized by the 100 Å periodicity represent membranes with a symmetric distribution of cytochrome b_5 on both sides of the bilayer. If an extent of 30 Å (as projected onto the profile axis) is assumed for the heme peptide of cytochrome b_5 (7) and a width of 45 Å is assumed for the lipid bilayer, then the expected periodicity for a symmetric membrane would be 105 Å, which is observed in some of our diffraction patterns. A residual asymmetry retained by such membranes, with slightly more cytochrome on the side of the membrane corresponding to the external surface of the collapsed membrane vesicles than on the side corresponding to the internal space, would then result in a unit cell of ~210 Å, with the weak odd orders such as the case where $I(h = 1)$ is observed (Fig. 8). Alternatively, an asymmetric positioning of the membrane within the water layers would produce a similar diffraction pattern. Although odd orders higher than $h = 1$ were not detected in the x-ray diffraction patterns (in contrast to the neutron diffraction patterns obtained by Gogol et al. [12], where the intensities of the odd orders were comparable to those of the even orders), this discrepancy may result from the differences in relative x-ray vs. neutron density contrast between components of the unit cell. Moreover, if the lipid bilayers of the 200 Å unit cell repeat obtained by Gogol et al. are positioned at the center of each half-unit cell (i.e., at $x = D/4$), then it is difficult to construct a physical model where cytochrome b_5 is asymmetrically inserted into the membrane. Such a model would require a large water space between the lipid bilayers at the center of the unit cell, whereas the space containing the heme peptide at the edges of the cell would be substantially condensed; this latter constraint seems unlikely at the low humidities used by these workers. For these reasons, and since our diffraction data suggest that membrane multilayers with 100 and 200 Å periodicities have a large degree of symmetry, it is likely that membrane multilayers with a unit cell repeat of 145–175 Å represent membranes that retain full asymmetry (as indicated by the low- and high-resolution electron density profiles of Fig. 6), whereas membranes with a repeat of 100 or 200 Å have undergone a degree of rearrangement to form a more symmetrical structure.

We gratefully acknowledge the assistance of Dr. T. MacAlister, Director of the Electron Microscope Facility, and Susan Lukas for protein purification. Many thanks to Ms. T. Daigle for typing the manuscript. Dr. Herbette is a Charles E. Culpepper Foundation Fellow and an Established Investigator of the American Heart Association.

The research was supported by research grants GM-15924, HL32588, HL-21812, and HL-22135 from the National Institutes of Health and by a grant from the American Heart Association and its Connecticut Affiliate.

Received for publication 23 April 1985 and in final form 12 November 1985.

REFERENCES

1. Holloway, P. W., and S. J. Wakil. 1970. Requirement for reduced diphosphopyridine nucleotide-cytochrome b_5 reductase in stearyl coenzyme A desaturation. *J. Biol. Chem.* 245:1862–1865.
2. Hildebrand, A., and R. W. Estabrook. 1971. Evidence for the participation of cytochrome b_5 in hepatic microsomal mixed-function oxidation reactions. *Arch. Biochem. Biophys.* 143:66–79.
3. Okayasu, T., T. Ono, K. Shinojima, and Y. Imai. 1977. Involvement of cytochrome b_5 in oxidative desaturation of linoleic acid to γ-linolenic acid in rat liver microsomes. *Lipids.* 12:267–271.
4. Reddy, V. R., P. Kupfer, and E. Caspi. 1977. Mechanism of C-5 double bond introduction in the biosynthesis of cholesterol by rat liver microsomes. *J. Biol. Chem.* 252:2797–2801.
5. Paultanf, F., R. A. Prough, B. S. S. Masters, and J. M. Johnston. 1974. Evidence for the participation of cytochrome b_5 in plasmalogen biosynthesis. *J. Biol. Chem.* 249:2661–2662.
6. Keyes, S. R., J. A. Alfano, I. Jansson, and D. L. Cinti. 1979. Rat liver microsomal elongation of fatty acids. Possible involvement of cytochrome b_5. *J. Biol. Chem.* 254:7778–7784.
7. Mathews, F. S., and E. W. Czerwinski. 1976. Cytochrome b_5 and cytochrome b_5 reductase from a chemical and x-ray diffraction point of view. *In* Enzymes of Mammalian Cell Membranes. A. N. Martonosi, editor. Plenum Publishing Corp., New York. 4:143–505.
8. Strittmatter, P., and H. A. Dailey. 1982. Essential structure features and orientation of cytochrome b_5 in membranes. *In* Membranes and Transport. A. N. Martonosi, editor. Plenum Publishing Corp., New York 1:71–82.
9. Dailey, H. A., and P. Strittmatter. 1981. Orientation of the carboxyl and NH_2 termini of the membrane-binding segment of cytochrome b_5 on the same side of phospholipid bilayers. *J. Biol. Chem.* 256:3951–3955.
10. Takagaki, Y., R. Radhakrishnan, C. Gupta, and H. G. Khorana. 1983. The membrane-embedded segment of cytochrome b_5 as studied by cross-linking with photoactivatable phospholipids. I. The transferable form. *J. Biol. Chem.* 258:9128–9135.
11. Takagaki, Y., R. Radhakrishnan, K. W. A. Wirtz, and H. G. Khorana. 1983. The membrane-embedded segment of cytochrome b_5 as studied by cross-linking with photoactivatable phospholipids. II. The nontransferable form. *J. Biol. Chem.* 258:9136–9142.
12. Gogol, E. P., D. M. Engelman, and G. Zaccai. 1983. Neutron diffraction analysis of cytochrome b_5 reconstituted in deuterated lipid multilayers. *Biophys. J.* 43:285–292.
13. Gogol, E. P., and D. M. Engelman. 1984. Neutron scattering shows that cytochrome b_5 penetrates deeply into the lipid bilayer. *Biophys. J.* 46:491–495.
14. Strittmatter, P., P. Fleming, M. Connors, and D. Corcoran. 1978. Purification of cytochrome b_5. *Methods Enzymol.* 52:97–101.
15. Spatz, L., and P. Strittmatter. 1971. A form of cytochrome b_5 that contains an additional hydrophobic sequence of 40 amino acid residues. *Proc. Natl. Acad. Sci. USA.* 68:1042–1046.
16. Shafer, D. A., and D. E. Hultquist. 1980. Purification of bovine liver microsomal NADH-cytochrome b_5 reductase using affinity chromatography. *Biochem. Biophys. Res. Commun.* 95:381–387.
17. Bangham, A. D., M. W. Hill, and N. G. A. Miller. 1974. Preparation and use of liposomes as models of biological membranes. *Methods Membr. Biol.* 1:1–68.
18. Singleton, W. S., M. S. Grey, M. L. Brown, and J. L. White. 1965. Chromatographically homogeneous lecithin from egg phospholipids. *J. Am. Oil Chem. Soc.* 42:53–56.

19. Chen, P. S., T. Y. Toribana, and W. Huber. 1956. Microdetermination of phosphorus. *Anal. Chem.* 28:1756–1758.
20. Enoch, H. G., and P. Strittmatter. 1977. Formation and properties of 1000Å-diameter, single-bilayer phospholipid vesicles. *Proc. Natl. Acad. Sci. USA.* 76:145–149.
21. Herbette, L., A. Scarpa, J. K. Blasie, C. T. Wang, A. Saito, and S. Fleischer. 1981. A comparison of the profile structures of isolated and reconstituted sarcoplasmic reticulum membranes. *Biophys. J.* 36:47–72.
22. Herbette, L., T. MacAlister, T. F. Ashavaid, and R. A. Colvin. 1985. Structure-function studies of canine cardiac sarcolemmal membranes. II. Structure organization of the sarcolemmal membrane as determined by electron microscopy and lamellar x-ray diffraction. *Biochim. Biophys. Acta.* 812:609–623.
23. Herbette, L., J. Marquardt, A. Scarpa, and J. K. Blasie. 1977. A direct analysis of lamellar x-ray diffraction from hydrated oriented multilayers of fully functional sarcoplasmic reticulum. *Biophys. J.* 20:245–272.
24. Herbette, L., P. DeFoor, S. Fleischer, D. Pascolini, and J. K. Blasie. 1985. The separate profile structures of the functional calcium and the phospholipid bilayer within isolated sarcoplasmic reticulum membranes determined by x-ray and neutron diffraction. *Biochim. Biophys. Acta.* 817:103–122.
25. Blasie, J. K., L. Herbette, D. Pascolini, V. Skita, D. H. Pierce, and A. Scarpa. 1985. Time resolved x-ray diffraction studies of the sarcoplasmic reticulum membrane during active transport. *Biophys. J.* 48:9-18.
26. Conte, S. D., and C. De Book. 1972. Elementary Numerical Analysis. McGraw-Hill, Inc., New York. 233–240.
27. Schwartz, S., J. E. Cain, E. A. Dratz, and J. K. Blasie. 1975. An analysis of lamellar x-ray diffraction from disordered membrane multilayers with application to data from retinal rod outer segments. *Biophys. J.* 15:1201–1233.
28. Moody, M. F. 1963. X-ray diffraction pattern of nerve myelin: a method for determining the phases. *Science (Wash. DC).* 142:1173–1174.
29. Stamatoff, J. B., and S. Krimm. 1976. Phase determination of x-ray reflections for membrane-type systems with constant fluid density. *Biophys. J.* 16:503–516.
30. Guiner, A. 1963. X-Ray Diffraction. W. H. Freeman, San Francisco, CA. 378 pp.
31. Cohn, E. J., and J. T. Edsall. 1943. Density and apparent specific volume of proteins. *In* Proteins, Amino Acids and Peptides. E. J. Cohn and J. T. Edsall, editors. Reinhold Publishing Corp., New York. 370–381.
32. Fleming, P. J., H. A. Dailey, D. Corcoran, and P. Strittmatter. 1978. The primary structure of the nonpolar segment of bovine cytochrome b_5. *J. Biol. Chem.* 253:5369–5372.
33. Blaurock, A. E. 1972. Structure of the retinal membrane containing the visual pigments. *Adv. Exp. Med. Biol.* 24:53–63.
34. Huang, C., and J. T. Mason. 1978. Geometric packing constraints in egg phosphatidylcholine vesicles. *Proc. Natl. Acad. Sci. USA.* 75:308–310.
35. Brady, G. W., D. B. Fein, M. E. Harder, and G. Meissner. 1982. Liquid diffraction analysis of sarcoplasmic reticulum. *Biophys. J.* 37:637–645.
36. Enoch, H. G., P. J. Fleming, and P. Strittmatter. 1979. The binding of cytochrome b_5 to phospholipid vesicles and biological membranes. *J. Biol. Chem.* 254:6483–6488.
37. Dailey, H. A., and P. Strittmatter. 1981. The role of COOH-terminal anionic residues in binding cytochrome b_5 to phospholipid vesicles and biological membranes. *J. Biol. Chem.* 256:1677–1680.
38. Blaurock, A. E. 1973. The structure of a lipid-cytochrome *c* membrane. *Biophys. J.* 13:290–298.
39. Pachence, J. M., P. L. Dutton, and J. K. Blasie. 1983. A structural investigation of cytochrome *c* binding to photosynthetic reaction centers in reconstituted membranes. *Biochim. Biophys. Acta.* 724:6–19.
40. Fleming, P. J., D. E. Koppel, A. L. Y. Lau, and P. Strittmatter. 1979. Intramembrane position of the fluorescent tryptophanyl residue in membrane-bound cytochrome b_5. *Biochemistry.* 18:5458–5464.
41. Dailey, H. A., and P. Strittmatter. 1978. Structural and functional properties of the membrane binding segment of cytochrome b_5. *J. Biol. Chem.* 253:8203–8209.